Lithium Abundances in Asymptotic Giant Branch Stars

Julie A. Krugler
Department of Physics & Astronomy, Michigan State University, East Lansing, MI 48824-1116
kruglerj@msu.edu

ABSTRACT

When stars undergo helium shell burning, they are subject to many different mixing processes which contribute to unusual elemental abundances found in these stars. ^{7}Lithium burns at relatively low temperatures; however, it is found in these asymptotic giant branch (AGB) stars. This should not be possible, except through the production of lithium via hot bottom burning and the Cameron-Fowler mechanism. In this study, 122 AGB candidates were analyzed for possible lithium production. Lithium abundances (or upper limits) were determined for these stars using MOOG, as well as [Fe/H] and rotational velocity estimates.

Subject headings: stars: Abundances –stars: Asymptotic Giant Branch Stars

1. Introduction

The understanding of the abundance of lithium in stars is an important key to understanding the chemical nature of the universe. Lithium is one of the three elements that were produced in the Big Bang; lithium is also an integral part of the proton-proton chain. Lithium is continually destroyed throughout the lifetime of a star. Even before a star enters the main sequence, convection dilutes the primal lithium from the surface of the star where it is eventually burned deeper inside the star through the proton-proton (PP) chain. Lithium is also destroyed in PPII as the final stage of helium production. As a star ascends the RGB, what little lithium is left at the surface is convected away from the surface, making these stars highly lithium deficient. By the time a star enters the AGB, there should essentially be zero lithium; however, this is not necessarily the case.

There have been many studies about the abundance of lithium in stars because its primary feature is at an accessible area of the spectrum and can be easily identified. The studies usually involve dwarf stars or stars on the red giant branch; extensive surveys of the lithium abundance in AGB stars have not really been conducted to date. Studies of the lithium content of giant stars have been conducted (Charbonnel & Balachandran 2000, Luck & Lambert 1982, Lebre et al. 2006); however, the majority of the stars in these studies have been on the red giant branch, as opposed to the AGB. One of the intentions of this study is to populate a previously under-sampled region of the H-R diagram.

The AGB is a fairly inaccessible region of the H-R diagram because it's difficult to ascertain that stars are indeed on the AGB. Luminosities must be known, which is not an easy task due to the uncertainty that arises in distance calculations. Despite the difficulties, it is important to understand these stars, as they provide observable clues to the inside of their cores given their highly convective envelope. This convection allows for material in the core of the star to be brought to the surface and often causes hot bottom burning where the bottom of the convective envelope of the star begins to undergo hydrogen to helium fusion. It also works to enable the Cameron-Fowler mechanism which is responsible for the production of lithium in these AGB stars.

In the PPII and PPIII, ^{7}Be is one in a step of many to form alpha particles. ^{7}Be can gain a proton to become ^{8}B and complete PPIII, or it can gain an electron to form ^{7}Li and complete PPII. In order for ^{7}Be to gain a proton, the temperature must be sufficiently high. In the Cameron-Fowler

transport mechanism ^{7}Be is taken from a hot region in the star to a cooler region where it's only able to capture protons. This facilitates the production of ^{7}Li and serves as an explanation of the lithium detections in AGB stars.

In this analysis, 122 AGB stars are studied to attain metallicities, v sin i, and the lithium abundance. Thirty-seven positive detections were found, with log ϵ Li values ranging from 1.22 to -1.1.

2. Observations

122 stars were observed between three observatories. 92 stars were observed at McDonald Observatory on the 2.1m telescope using the Sandiford Cassegrain Echelle Spectrometer. 16 stars were observed at the European Southern Observatory using the Fiber-fed Extended Range Optical Spectrograph (FEROS) Instrument on the 1.52m telescope. 16 stars were also observed at the Hauteprovedce Observatory using the 1.52m telescope with the Aurelie Spectrometer.

2.1. Data Reduction

McDonald and FEROS data were reduced in IRAF using the echelle, rv, and onedspec packages. Aurelie data were reduced using MIDAS.

Instrument independent data are necessary to calculate abundances, as well as to enable the observer to compare data taken with different instruments. In echelle spectroscopy, instrument independence is maintained by removing the Blaze function of the echelle, which differs from instrument to instrument; this process is known as normalization. Normalization of the spectra was carried out by the splot routine for all the McDonald and FEROS spectra. Aurelie data were reduced using MIDAS. A fit of a hot star was made for each instrument for each night. Cool stars with strong TiO bandheads were often fit using the the hot star fits because the continuum was engulfed.

3. Abundance Analysis of Lithium

The MOOG software (Sneden 1973) was used to perform abundance calculations of lithium. MOOG requires a parameter file which includes an atmospheric model, a line list, and the normalized spectrum.

3.1. Atmospheric Models

Atmospheric models were created using Kurucz and MARCS models. They required the effective temperature, surface gravity, and microturbulence. They also required the overall metallicity of the star in the form of [Fe/H]. Kurucz models were used for stars without significant TiO. In general, the coolest stars with Kurucz models were around 3950 K. They were also made specifically for each star. MARCS models were much more appropriate for cooler stars, as they accounted for line blanketing caused by the TiO, whereas the Kurucz models did not. MARCS models were not made to be star specific; rather a matrix of models was used.

3.2. Stellar Parameters

3.2.1. Effective Temperature

The lithium line is notoriously temperature sensitive. It is crucial to attain a correct value for the effective temperature of the star. First guess effective temperatures were based on the Ramirez & Melendez (2005) paper for a temperature scale for FGK stars. Temperatures were determined by the V-I, V-J, and V-K colors, with the median being taken as the value. V and I magnitudes were known for these stars and the J and K colors were taken from the 2MASS catalog. An extensive literature search was also conducted to find other effective temperature estimates for the program stars. When available, the literature temperatures were used if the calculated temperatures were clearly wrong for the star.

Reddening is essential to photometric determination of effective temperatures. It provided a problem with many of the stars. The Schelgal (1998) dust maps were used as an indicator of reddening; however, given its notable problem with the overestimation of the reddening of disk stars, Neckel (1980) or Savage (1985) reddening estimates were used when available.

The final determination of effective temperature was conducted through iteration using MOOG. For hotter stars, the exact temperature calculated (or quoted from the literature) was used as a first guess for the effective temperature; for cooler stars, a matrix of models was used, with the temperature being forced to the closest avail-

able in the matrix. Five iron lines in the lithium region were used as an indicator of the temperature. They all had differing oscillator strengths, which corresponded differently to incorrect temperatures.

The uncertainties associated with effective temperature were assigned to be 100K given that the reddening was not always correct. This temperature effect corresponded to the largest source of error determined in the lithium abundance.

3.2.2. Surface Gravity

The surface gravity, log g, was derived from first principles where

$$g = \left(\frac{GM}{r^2}\right) \tag{1}$$

and

$$L = 4\pi r^2 \sigma T^4 \tag{2}$$

which can be rearranged to produce

$$r^2 = \left(\frac{L}{4\pi\sigma T^4}\right). \tag{3}$$

This equation (2) can then be substituted in the first equation giving the following:

$$g = \left(\frac{4GM\pi\sigma T^4}{L}\right). \tag{4}$$

Surface gravity, much like [Fe/H], is really computed in comparison to the solar value, so constants G, π, σ, and 4 drop out of the equation leaving

$$\left(\frac{g}{g_o}\right) = \left(\frac{\left(\frac{M}{M_o}\right)\left(\frac{T^4}{T_o^4}\right)}{\left(\frac{L}{L_o}\right)}\right). \tag{5}$$

In the final step of the derivation, surface gravity is actually taken as a logarithm in the atmospheric models given its large values. The final form of surface gravity was:

$$logg = logg_o + 4log\left(\frac{T}{T_o}\right) + log\left(\frac{M}{M_o}\right) + log\left(\frac{L_o}{L}\right). \tag{6}$$

The uncertainties associated with the surface gravity relied most heavily upon the uncertainties in the luminosity. This produced an error of 0.4.

3.2.3. Microturbulence

Microturbulence is a way to account for the turbulent stellar atmosphere. Line broadening that cannot be attributed to other factors (e.g. rotational velocity) is attributed to the microturbulence of the star. Microturbulence was derived from the relation of microturbulence and surface gravity in Smith et al. (1995).

$$v_t = -0.249466(logg) + 1.71526 \tag{7}$$

The imprecise nature of the determination of the microturbulence reflects the relative importance of the parameter. Surface gravity was more important than microturbulence; however, temperature was much more important than surface gravity and was proved to be so in error analysis. Errors were assumed to be 0.5 km/s.

3.2.4. Metallicity

Metallicities were taken from a literature search. When no metallicity was available, [Fe/H] was initially assumed to be solar. Metallicity was adjusted through MOOG, using the New Abundances option. For changes in [Fe/H] greater than or equal to 0.1 dex, another model was used with the corresponding change in metallicity. Lithium is a metallicity sensitive line; there is also a strong iron feature near the lithium line with which it is often blended. It is therefore essential to correctly match the metallicity. This was done through matching several nearby Fe I lines in the spectrum.

3.3. Spectral Synthesis

Given the parameters required to run MOOG, synthetic spectra were created. This was the vehicle through which the lithium abundance was determined. The fit of the lithium line determined the abundance. However, the stellar parameters must first be correct and the abundance of C, Fe, and Ti are crucial to correctly fitting the region. The shift in velocity must be accounted for as well. This is trivial in MOOG because there is an option that allows the user to shift the normalized spectrum to match the rest wavelengths of the features of the synthetic spectrum. However, calculating the rotational and radial velocities of the star, which necessitate the shift, is a nontrivial

process that has been performed on only a subset of the stars.

Iron is important to correctly synthesize because it accounts for the overall metallicity of the star as well as shaping the lithium region. TiO molecules swamp the area in cool stars, beginning at about 3800 K, and essentially destroy the continuum. Adjusting the Ti is important so that the features are well matched. Carbon also plays an important role. In hot stars, the C_2 feature can dominate the lithium region. In cooler stars, the carbon must be adjusted to ensure proper TiO abundances. High carbon abundances in cool stars creates CO, which depletes the available oxygen to form TiO.

4. Velocity Calculations

Rotational velocities were computed for all of the stars, whilst radial velocities were computed for the McDonald stars. The rv package in IRAF was utilized. The fxcor routine was used to ascertain full width half maximums (FWHM), heliocentric velocities, and error estimates on the heliocentric velocities. The rotational velocities, which correspond to the rotation of the star itself, were calculated using the smallest FWHM per each instrument as follows:

$$v_{rot} = \sqrt{FWHM^2_{star} - SFWHM^2} \qquad (8)$$

where the SFWHM is the smallest recorded FWHM taken at an instrument and $FWHM_{star}$ is the FWHM of the star. This method does not account well for rotational velocities below about 5 km/s. The v_{rot} is obviously wrong for the smallest FWHM of the set and is better understood as an upper limit for all v_{rot} less than 5 km/s.

Radial velocities were computed by using the rvcorrect routine. It was only performed on the McDonald data because those were the only stars with complete header files which included right ascension, declination, and the UT at which the exposure was taken. Without this information it is not possible to complete the calculation. The values computed by rvcorrect must be added to the heliocentric velocity to account for the earth's motion around the sun. This is the actual radial velocity computed for the star. Aurelie and FEROS data did not include the aforementioned information and computation of these stars is to be completed in the future.

5. Results

Of the 122 stars, 37 positive lithium detections were found. Log ϵ values ranged between 1.22 and -1.10 dex. As effective temperature goes up, the ability to detect lithium and establish upper limits goes up. This is due to the temperature sensitivity of the lithium line; as the temperature increases, the line weakens. High S/N with high resolution is required to determine abundances in hot stars with weak lithium, but this is extremely difficult to do, given that high resolution reduces the S/N.

The largest source of error was due to effective temperature. Errors in effective temperature caused the abundances to vary by +0.17 and -0.2 in the population of stars hotter than 3900. For the cooler stars, errors of +0.25 and -0.3 were more appropriate because the temperatures were even more uncertain given the difficulty fitting the TiO continuum. Changes in surface gravity and mircoturbulence did not change the value of the lithium line. This should be expected because changes in surface gravity really only effect the comparison of ionized species of elements. The lithium here was ^{7}Li. The resolution of the data was not high enough to really distinguish between ^{6}Li and ^{7}Li. Microturbulence was also not expected to play a huge role in error analysis because of its relatively small contribution to the synthetic spectrum.

In recent papers (Lebre et al. 2006) it has been suggested that rotational velocity and the lithium abundance are linked. However, in this data set, there are no correlations to be found in rotational velocity and log ϵ Li. Data were scattered with abundances having high and low rotation. The upper limits were similarly scattered. Though this does not support the studies linking rotation and lithium abundances, this also does not negate the work. Errors are sufficiently high enough on the rotational velocities to question the validity of the numbers. A link between metallicity and lithium abundance has also been suggested. However, this is also not seen in this data set.

6. Conclusions

The objective of this project was to analyze 122 AGB stars for lithium abundance; this has been

accomplished with 37 stars yielding positively for the detection of lithium. An increase in the population of a previously undersampled region of the H-R diagram has been achieved. Future work on this project could include calculations of the carbon isoptic ratio of these AGB stars, as well as the completion of the radial velocity calculation for the Aurelie and FEROS data.

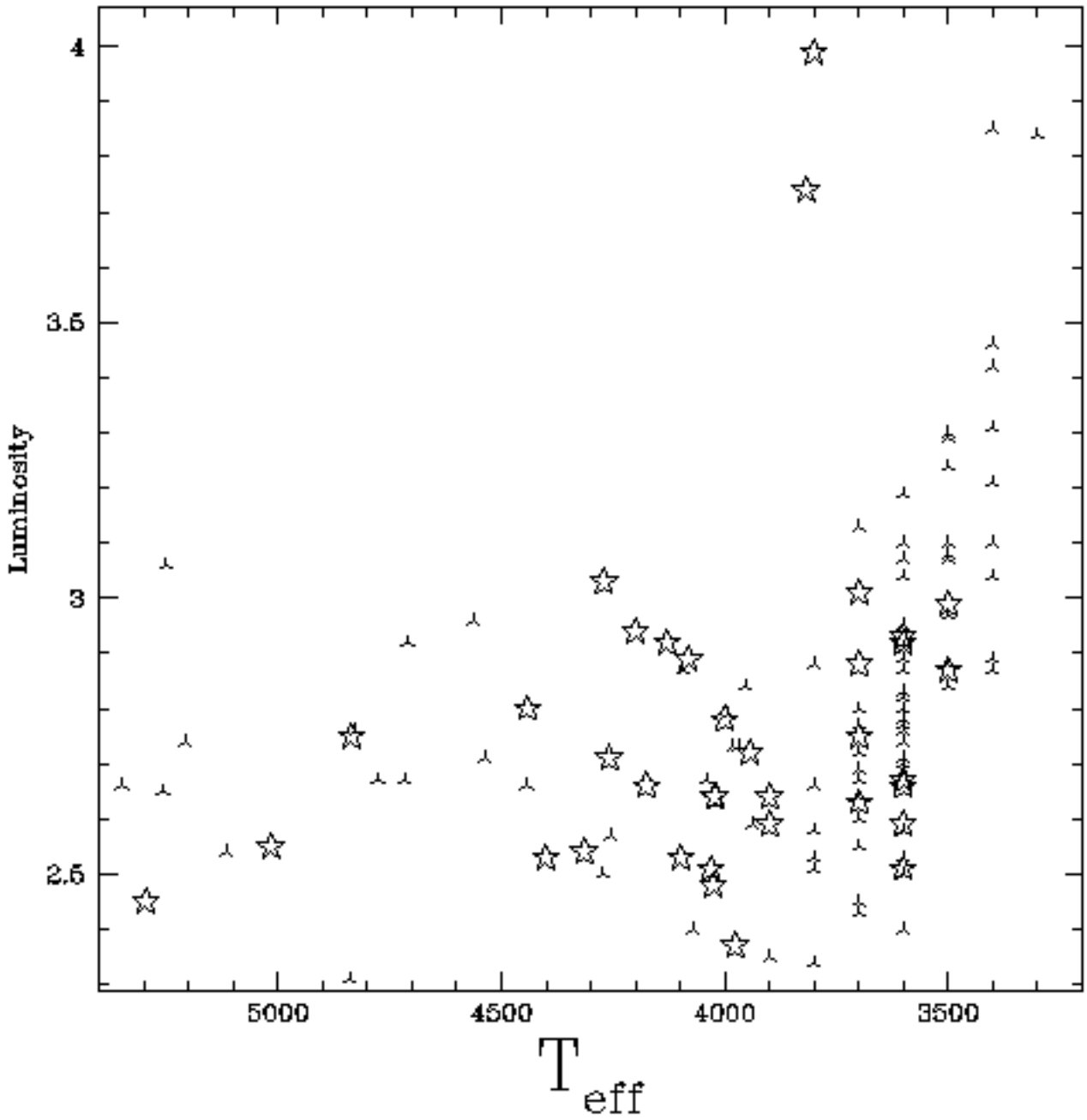

Fig. 1.— H-R Diagram of the program stars. Open stars are abundances and the other symbol indicates an upper limit.

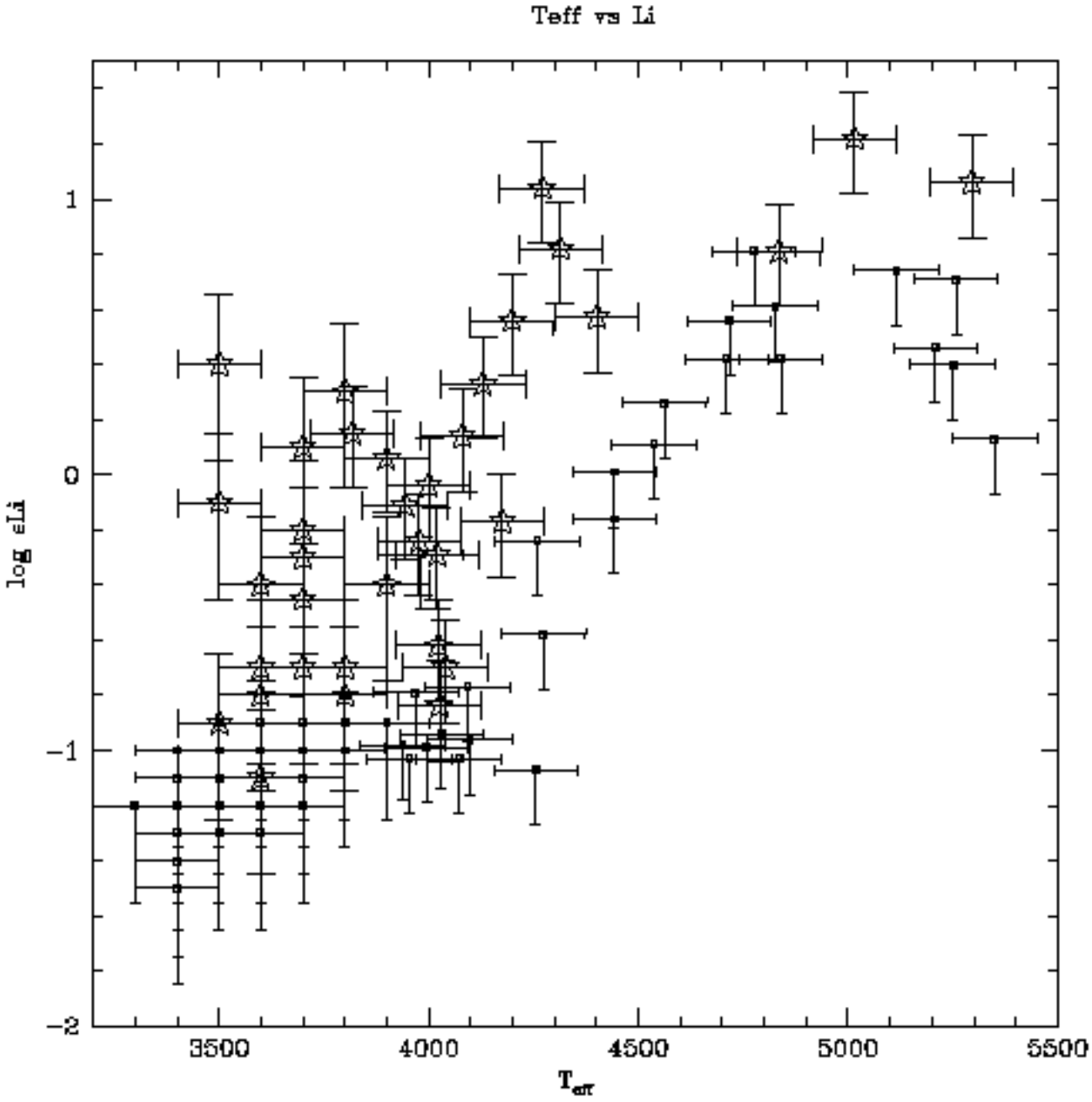

Fig. 2.— Plot of the lithium abundances and upper limits versus the effective temperature. Abundances appear as open stars.

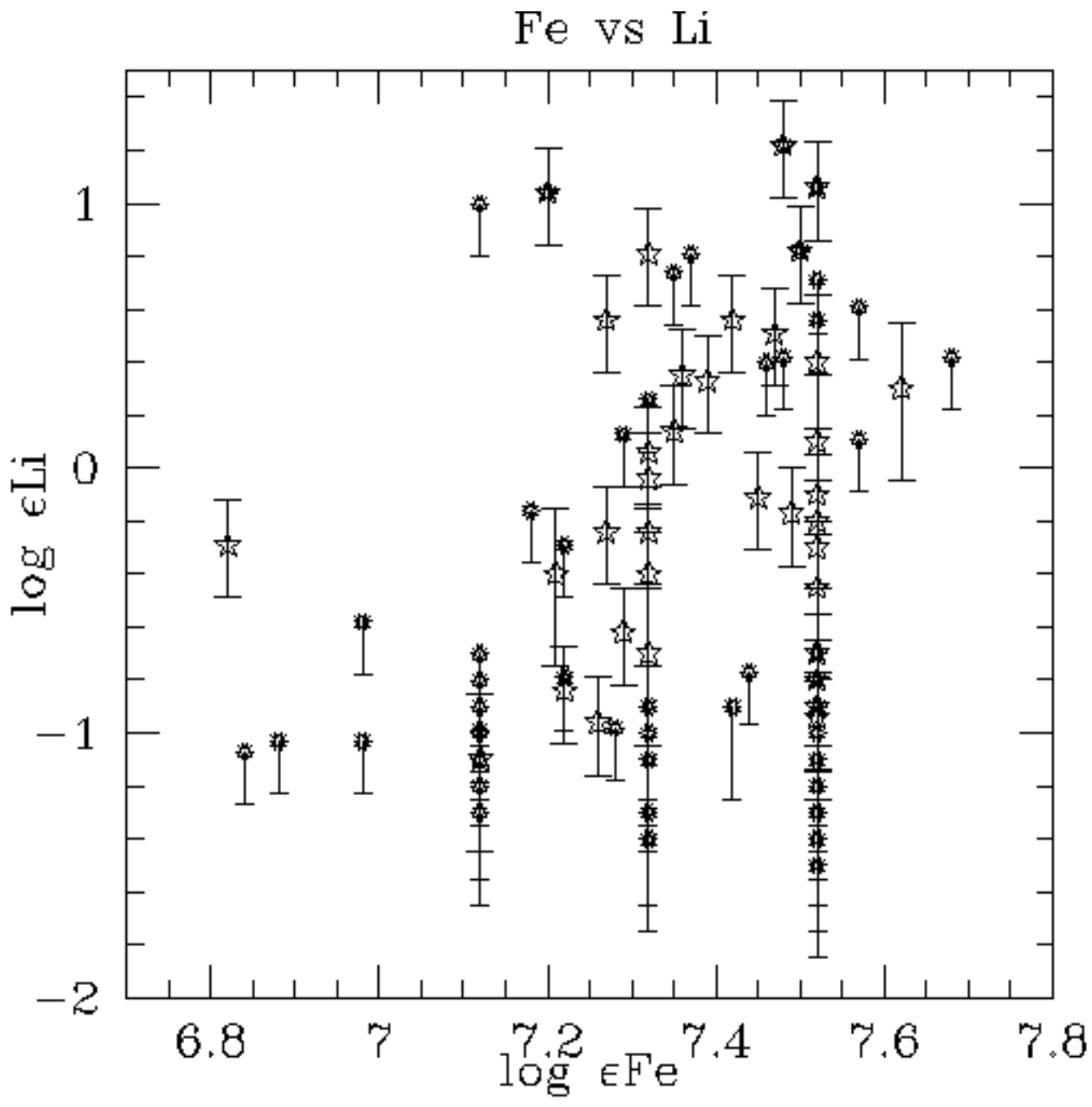

Fig. 3.— Plot of the log ϵ Li value versus the log ϵ Fe value. There is no obvious correlation between the two parameters. Abundances appear as open stars.

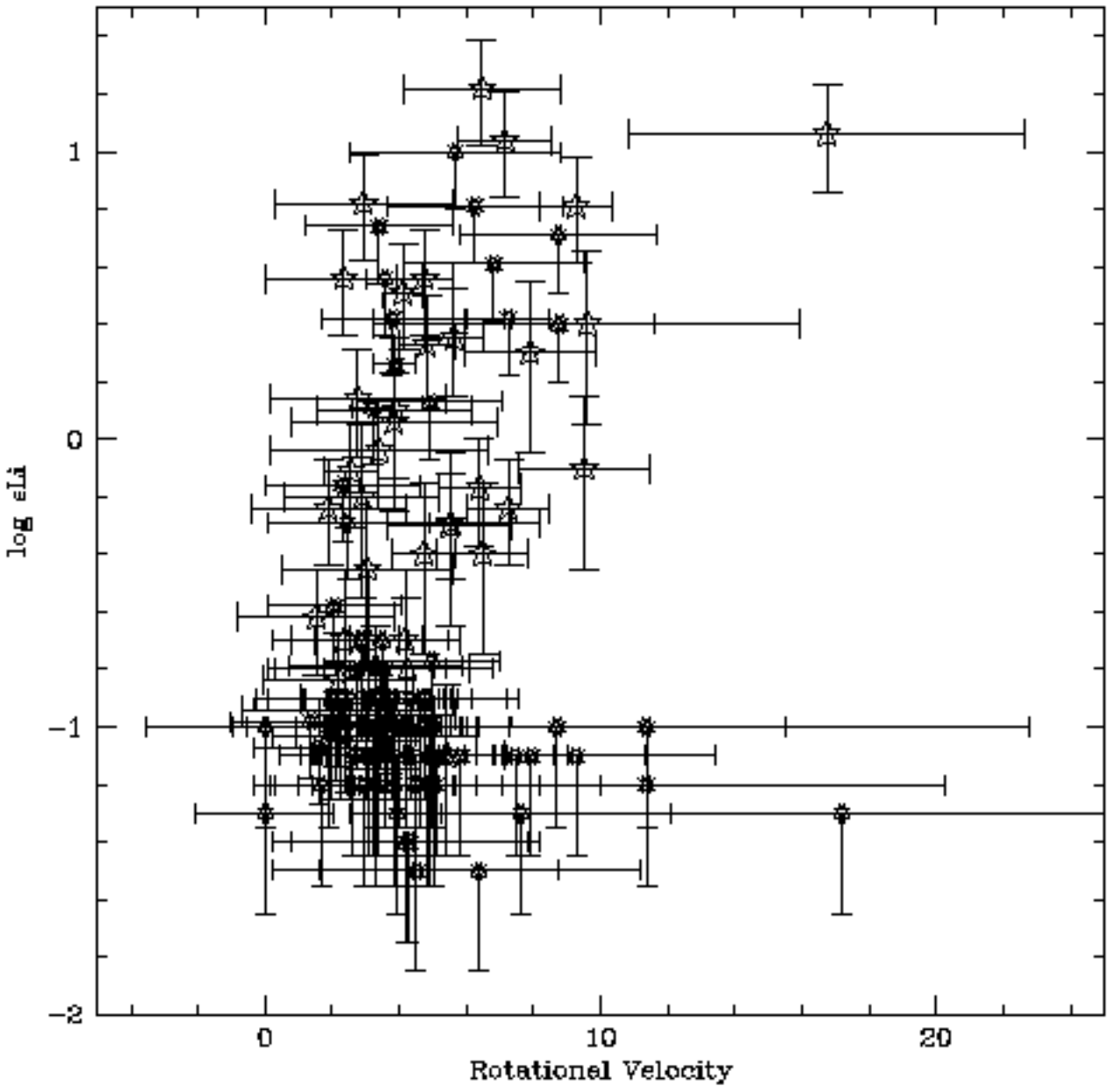

Fig. 4.— Plot of the log ϵ Li value versus the rotational velocity value. Again, there is no obvious correlation between the two parameters. Abundances appear as open stars.

7. Bibliography

Cameron, A. G. W.; Fowler, W. A., 1971, Ap. J., 164, 111C.
Charbonnel, C., Balachandran, S. C., 2000, AandA 359, 563C.
do Nascimento, J. D., Jr., et al., 2000, AandA, 357, 931D.
Karakas, A., Ph.D. Thesis 2003.
Lebre, A., et al. 2006, AandA, 450, 1173L.
Luck, R. E., and Luck, D.L. 1982, *Ap.J.*, 256, 189.